Microsyst Technol (2011) 17:1755–1762
DOI 10.1007/s00542-011-1356-1

TECHNICAL PAPER

Structural, morphological and micromechanical studies on fly ash reinforced PMMA composites

Arunendra Kumar Patel · R. Bajpai · J. M. Keller · Bindu Kumari · V. Vatsal · A. Saha

Received: 6 August 2011 / Accepted: 14 September 2011 / Published online: 1 October 2011

Abstract This paper is focused on the study of the structural, morphological, mechanical and microhardness studies on Fly ash reinforced PMMA composites. Fly ash reinforced PMMA composites have been prepared with the sol–gel method. Fourier transformed infrared (FT-IR) spectroscopy, X-ray diffraction, microhardness and atomic force microscopy (AFM) studies have been done on prepared composite. The AFM images confirm the presence of fly ash particles in nanophase within the PMMA matrix. The crystalline size of the in situ generated nanoparticles was investigated with X-ray diffraction technique and it is found that the crystallinity index increases with increasing the concentration of the fly ash. The structural characterization has been done with FT-IR spectroscopy. The FT-IR spectra of pure PMMA and fly ash based composites has been observed and analyzed. The Vickers microhardness indentation technique has been employed to detect the effect of reinforcement of fly ash in the PMMA matrix. Significant changes were observed in the various properties of the fly ash reinforced PMMA composites.

A. K. Patel (✉) · R. Bajpai · J. M. Keller · B. Kumari · V. Vatsal
Department of Physics and Electronics,
Rani Durgavati University, Jabalpur 482001, India
e-mail: patelarunendra@gmail.com

A. K. Patel · J. M. Keller
Macromolecular Research Centre (MRC),
Rani Durgavati University, Jabalpur 482001, India

A. Saha
UGC-DAE Consortium for Scientific Research, Kolkata Centre,
III/LB-8, Bidhannagar, Kolkata 700098, India

1 Introduction

Polymer composites play an important role in the preparation of new high performing polymeric materials for special applications (Celik et al. 2008; Chand and Vashishtha 2008; Dubey et al. 2008; Kumar et al. 2009). The Sol Gel process has been used to make the PMMA: fly ash composite, because this technique is the least expensive and best suited for fabrication of a variety of size, shape of composite (Guo and Rohatgi 1998). This method is versatile, strength forward and relatively inexpensive one for modifying the properties of polymer by adding the inorganic materials in it.

The major component of the fly ash are oxides (and mixed metal) oxides of silicon, aluminum, iron and calcium. Small amount of the oxides of other common elements such as magnesium and titanium are also present. The phases present were identified by X-ray diffraction as quartz, mullite, lime, spinel, hematite and ferrite (Celik et al. 2008; Kumar et al. 2009; Guo and Rohatgi 1998).

The matrix structure, processing and use of filler or reinforcement are the principle factors which affect mechanical, structural, thermal, electrical properties of polymer. The fly ash is one of the most important and inexpensive low density reinforcement available in large quantities as solid waste by product from combustion of coal in thermal power plants (Celik et al. 2008; Chand and Vashishtha 2008; Kumar et al. 2009; Guo and Rohatgi 1998). Hence the composites reinforced with fly ash are likely to overcome the cost barrier and reduce environmental hazard for the various useful applications. The Mechanical properties of the reinforced composites are affected by the size, shape and weight fraction of the reinforcement (Celik et al. 2008; Kumar et al. 2009; Guo and Rohatgi 1998).

The most important finding from the present study is the effect of addition of fly ash as filler/reinforcing material in

its structural, micromechanical and chemical compositional properties.

2 Experimental

2.1 Materials

For the preparation of the polymeric composite films, the commercially available polymer Poly(methyl methacrylate) obtained from BDH, UK, of molecular weight 5,00,000 and Fly Ash in powder form has procured from thermal plant, Singroli (M.P.) used without further purification, which were supplied by M/s Redox, Jabalpur.

2.2 Preparation of specimen

Fly ash in different concentrations was added to the fixed quantity of Poly(methyl methacrylate) to yield the composite of required concentration and designated as Pure PMMA Poly(methyl methacrylate), PC/FA (5), PI/FA (10), PI/FA (15) for 5, 10 and 15 weight percentage concentrations of fly ash respectively. The sol-gel method (Celik et al. 2008; Chand and Vashishtha 2008; Bajpai et al. 2002, 2003a, b; Gupta et al. 2007; Ramrakhiani et al. 2005) has been utilized to prepare the composite films of pure Poly(methyl methacrylate) and fly ash based composite films, dimethylformamide has been taken as solvent. Fly ash and Poly(methyl methacrylate) solution were mixed with the help of an electric motor operating at 200 rpm in air atmosphere at 60°C for 6 h. A Known quantity of the homogeneous solution poured in glass mould of size 4×4 cm^2 and kept in an electronic oven at 110°C temperature for 3 h. The oven was then switched off and the glass mould along with the solution was given sufficient time to cool down (nearly 24 h). Samples of 2 sq cm size and 0.05 cm thickness were cut from the pallets and kept in the air-tight polyethylene bags for further characterization.

2.3 FT-IR spectroscopy

The structural characterization of the pure Poly(methyl methacrylate), fly ash powder and their composites of various ratio were recorded with Perkin Elmer Spectrum BX-II equipment with resolution of 2 cm^{-1}.

2.4 Microhardness measurement

In the recent years the micro indentation technique of determining the microhardness has increasing use for the characterization of polymer, homopolymer, polymer blends, composite, biopolymer, copolymer (Dubey et al. 2008; Bajpai et al. 2002, 2003a, b; Gupta et al. 2007; Mishra et al. 2007). The microhardness studies has been carried out on pure Poly(methyl methacrylate) polymer and fly ash reinforced Poly(methyl methacrylate) composite films with the help of mhp160 micro hardness tester, equipped with the Vicker's diamond pyramidal indenter having a square base and 136° pyramidal angle attached to the Carl Zeiss NU2 Universal Research Microscope.

The Vicker hardness number (H_v) was calculated using the relation:

$$H_v = \frac{1.854 \times L}{d^2} \text{kg/mm}^2 \quad (1)$$

where L is the load (in kg.) and d is the diagonal of indentation (in mm). Indentations at each load were obtained in replicate number and average hardness number was calculated.

2.5 X-Ray diffraction

The X-ray diffraction technique is the most common technique used for the analysis of polymer system and analysis of material (Celik et al. 2008; Dubey et al. 2008; Kumar et al. 2009; Guo and Rohatgi 1998; Balamurugan et al. 2004; Bartram 1967; Ramrakhiani et al. 2005; Rizwan and Din 2004; Ma et al. 2009; Ron 2000; Statton 1967). The X-ray diffraction studies of prepared pure Poly(methyl methacrylate) polymer and fly ash reinforced Poly(methyl methacrylate) composites were carried out with the Bruker D8 Advance X-ray diffractometer, X-ray powder diffractometer with CuKα radiation (wave length 0.15405 nm) performed at 40 kV and 40 mA. The diffraction pattern is recorded in the 2θ range from 0° to 90° with scanning speed of 0.2° per minute.

The crystallinity has been measured on the premise that increasing amorphousness tends to broaden the line width whereas increasing crystallinity increases the intensity. The height (CrH) of the main peak above its adjacent minimum represents the crystallinity of the sample and the width (AmW) of the peak at this adjacent minimum is considered to represent the amorphousness of the sample. The crystallinity CrI, is calculated from the Eq. 2:

$$C_rI = \left[1 - t \times \frac{A_m W}{C_r H}\right] \quad (2)$$

where t is the scale factor relating the height of CrH to full scale (total blackness) (Statton 1967). From the diffraction patterns of the various samples, the interplaner distance d was computed for different peaks. Bragg's equation 3 was used to determine the distance between two successive planes from which the X-rays were diffracted:

$$2dSin\theta = n\lambda \quad (3)$$

where λ is the X-ray wavelength, θ is the Bragg's angle and n is the order of diffraction. d was calculated from the first

order (n = 1) for various peaks obtained in the diffraction patterns (Eq. 4):

$$d = \frac{\lambda}{2Sin\theta} \tag{4}$$

The relationship between the crystallite size and the X-ray line broadening was determined from the Scherrer's Equation:

$$D = \frac{k\lambda}{\beta Sin\theta} \tag{5}$$

where, D is crystallite size, λ is the wavelength, β is the angular line width of half maximum intensity, and θ is the Bragg's diffraction angle, k is the constant with a value of 0.89 (Dubey et al. 2008).

2.6 Morphological study

The surface topography was determined using an Atomic Force Microscopy (AFM) Nanoscope II from the Digital Instrument; in the contact mode and analysis was carried out using software (Version 2.2) available with the AFM.

3 Results and discussion

3.1 FT-IR spectroscopy

The FT-IR spectrum of pure PMMA (Fig. 1) indicates the details of functional groups present in the synthesized PMMA. The symmetric and asymmetric stretching of C–H in CH_3 is observed at 2,853 and 3,021 cm^{-1}. A sharp intense peak at 1,734 cm^{-1} appeared due to the presence of C=O stretching vibration, which confirms the presence of aldehyde group. The peak at 1,680 cm^{-1} shows the presence of solvent i.e. DMF. The symmetric and asymmetric stretching of the methyl (CH_3) group in one structural repeat unit have been observed at 3,021 and 2,987 and 2,802 and 2,732 cm^{-1}. The band at 1,148 cm^{-1} is assigned to the CH_3 twisting and wagging modes of CH_3 is presented at 1,198 cm^{-1}. The C=O in plane and out of plane bending is assigned at 750 cm^{-1}. The C–O in plane and out of plane bending in one structural repeat unit has been observed at 727 and 596 cm^{-1}. The medium C–C stretching is observed at 982 cm^{-1} (Deepa et al. 2002; Kalyanasundaram et al. 2001; Mas et al. 2010).

The FT-IR spectra of the fly ash are shown in Fig. 1. The result shows a broad band between 800 to 1,400 cm^{-1}. The three characteristic band peaks observed at 1,094, 563 cm^{-1}, a small peak at 3,448 cm^{-1} also appears which is due to symmetric and asymmetric stretching vibration of water bound. The 1,094 cm^{-1} peak is due to the higher concentration of SiO_2 (Si–O-Si) asymmetric and symmetric stretching vibration. The peak at 563 cm^{-1}, represents the presence Al–O vibration (Celik et al. 2008).

The FT-IR spectra of various concentrations have been taken. The formation of new peaks of fly ash with respect to the pure PMMA and shift in various peaks has been observed. For the 5 weight percentage concentration of fly ash, the peaks appeared at 1,057, 561 cm^{-1} representing SiO_2 asymmetric stretching vibration, and Al–O vibration respectively. The shifting in the peaks of characteristic frequency of PMMA with respect to pure PMMA is also observed at frequencies: 3,039 and 2,960 cm^{-1} representing the presence of symmetric and asymmetric stretches of methyl (CH_3), 2,858 cm^{-1} representing the symmetric stretching of C–H group, 1,731 cm^{-1} due to the presence of the C=O stretching vibrations. 1,146 cm^{-1} due to CH_3 twisting. 758 cm^{-1} due to C=O bending and 589 cm^{-1} due to C–O stretching. These shifts also have been observed for higher concentration composites.

3.2 Microhardness measurement

Microhardness of a material plays an important role on the chemical and morphological characteristics of material. Figure 2 illustrates the variation of microhardness (H_v) of pure PMMA and fly ash reinforced PMMA composite. The value of H_v is minimum for pure PMMA and increases with increasing concentration of fly ash. The graph also shows that the value of H_v increases curvilinearly with increasing load (10–80 gm), for different samples.

The increase in H_v with load is due to the strain hardening in the specimen. It is also noticed that the rate of strain hardening is grater at lower loads and lower at higher loads. The strain hardening phenomena in polymers can be explained on the basis of spectrum of micromodes of deformation in the polymer chain (Rabinowetz and Brown 1967). When sufficient number of micromodes becomes active, large scale plastic deformation begins. On applying load, the polymeric specimen is subjected to the strain hardening and as the load is increased, the specimen is subjected to the greater strain hardening and hence H_v increases. The final saturation value of H_v observed without illumination may be due to permanent deformation caused by chain–chain slipping in polymer composites. Vander Waals forces and relatively high molecular forces between the individual macromolecules are known to contribute to the strength of polymer (Bajpai and Datt 1986). The H_v attains a limiting value beyond the load at 50 g for the pure PMMA, 60 g for 5% fly ash reinforced fly ash composite and 70 g for 10 and 15% fly ash reinforced composites.

The different values of the microhardness at saturation for the pure PMMA and various incorporation of fly ash indicate the changes in macromolecular structure and

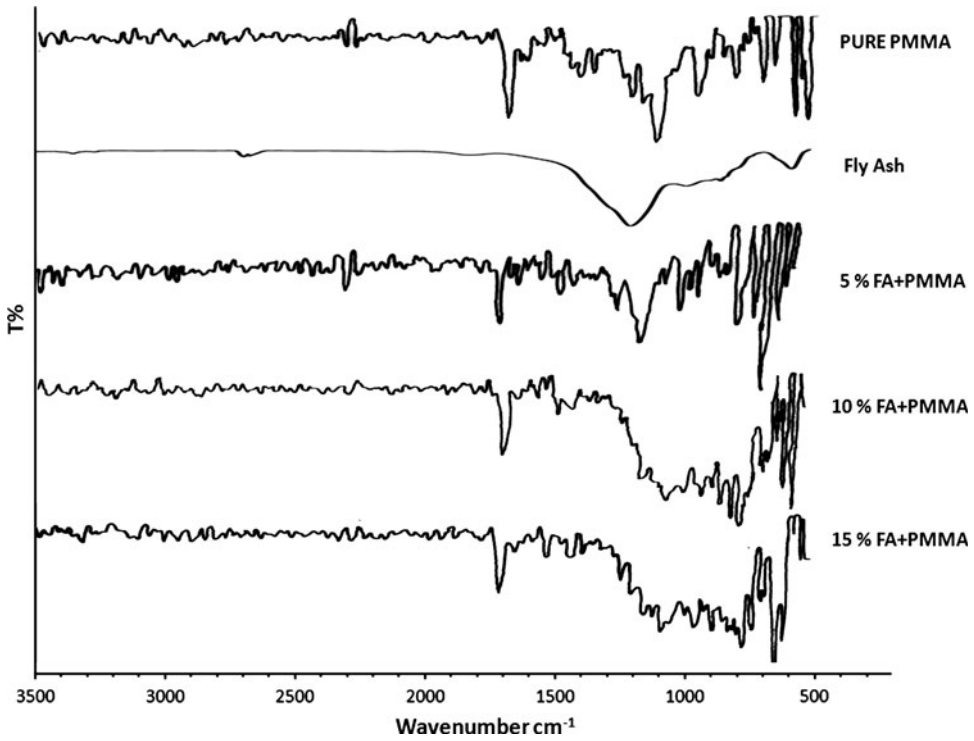

Fig. 1 FTIR analysis of pure PMMA, Fly Ash powder, 5% fly ash and PMMA, 10% fly ash and PMMA, 15% fly ash and PMMA

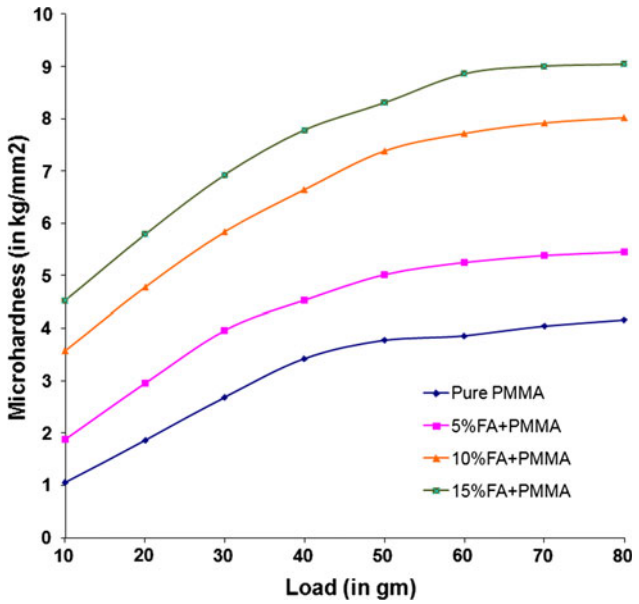

Fig. 2 Effect of load on the microhardness of pure PMMA, 5% fly ash and PMMA, 10% fly ash and PMMA, 15% fly ash and PMMA

morphology. On applying the load the polymer is subjected to some strain hardening. When H_v value tends to become constant, the polymer is completely strain hardened. The rate of strain hardening in various samples is related to weight percentage ratio of fly ash within the composite.

Figure 3 shows the effect of load (in g) on the variation of diagonal size (in mm) of pure PMMA, 5% fly ash and PMMA, 10% fly ash and PMMA, 15% fly ash and PMMA. The size of the diagonal decreases with increasing concentration of fly ash within PMMA matrix, which represent the increasing plasticization effect due to incorporation of the fly ash powder.

3.3 X-Ray diffraction

The structure and morphology is basically dependent upon regular arrangement of the atomic system or crystallinity. Polymers are in general amorphous or semi crystalline material. The crystallization of polymer depends on the degree of miscibility and mobility of the crystallizable and non crystallizable components in the specimen. The X-Ray pattern of pure PMMA, fly ash powder and fly ash reinforced PMMA composites are shown in Fig. 4. In all the samples based on the PMMA a broad peak observed between 12.85° to 13.85° and a narrow peak is also observed between 30.69° to 30.95°. The fly ash powder gives the first peak at 21.5° and 27°. In pure PMMA the first order diffraction peak is observed at 13.81° yielding CrI = 14.00% and second order peak observed at 31.04° which yields the CrI = 98.46%.

The powder of fly ash gives the first order diffraction peak at 21.5° and second order diffraction peak at 27.0° which gives the crystallinity index 96.71 and 96.61% respectively. Since the fly ash contains the SiO_2, Al_2O_3, $Ca(CO)_3$, Fe_2O_3, and other constituents, which contribute to crystalline phase, so the reinforcement of fly ash within PMMA matrix increases the crystallinity of the prepared

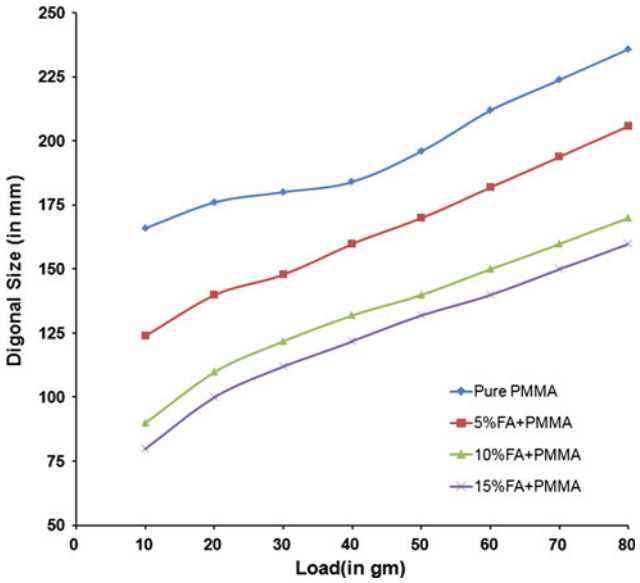

Fig. 3 Effect of load on the variation of diagonal size of pure PMMA, 5% fly ash and PMMA, 10% fly ash and PMMA, 15% fly ash and PMMA

composites. The crystallinity index suddenly increases from 14.00 to 43.04% for the 5 wt% concentration of fly ash in the PMMA matrix, the interplaner distance "d" also increases from 6.41 to 6.55 Å and crystallite size increases from 1.95 to 1.96 nm. These parameters also increase for 10 wt% as shown in the Table 1. The higher concentration of fly ash (15 weight percent) within PMMA matrix gives the crystallinity index 43.72%, interplaner distance 6.8489 Å and crystallite size as 9.87 nm.

3.4 Morphological study

The AFM results can give sufficient information on the surface morphology of pure PMMA and various FA/PMMA films. The AFM micrographs of the Pure PMMA and FA/PMMA films having different amount of fly ash are shown in Figs. 5, 6. It can be inferred from Fig. 5a that the surface has fairly smooth character, indicating planarized macromolecular chains is obtained for the Pure PMMA matrix. The change as the surface morphology with respect to the Pure PMMA is clearly evident from Fig. 5b–d for various FA/PMMA films. The incorporation of fly ash into the PMMA in different concentrations seems to development of nanostructures within the PMMA matrix (Fig. 5a, c). The distinctive domains with reasonable size and shape of fly ash within the PMMA matrix are obtained for various FA/PMMA composites. 3D- AFM image, reveals the dispersion of well organized fly ash domains within the PMMA matrix (Fig. 6a–d). Thus, the distribution of these well organized fly ash nanodomains within PMMA matrix may lead to enhancement of the micro-mechanical and crystallinity as compared to the pure PMMA (Fig. 7a, b).

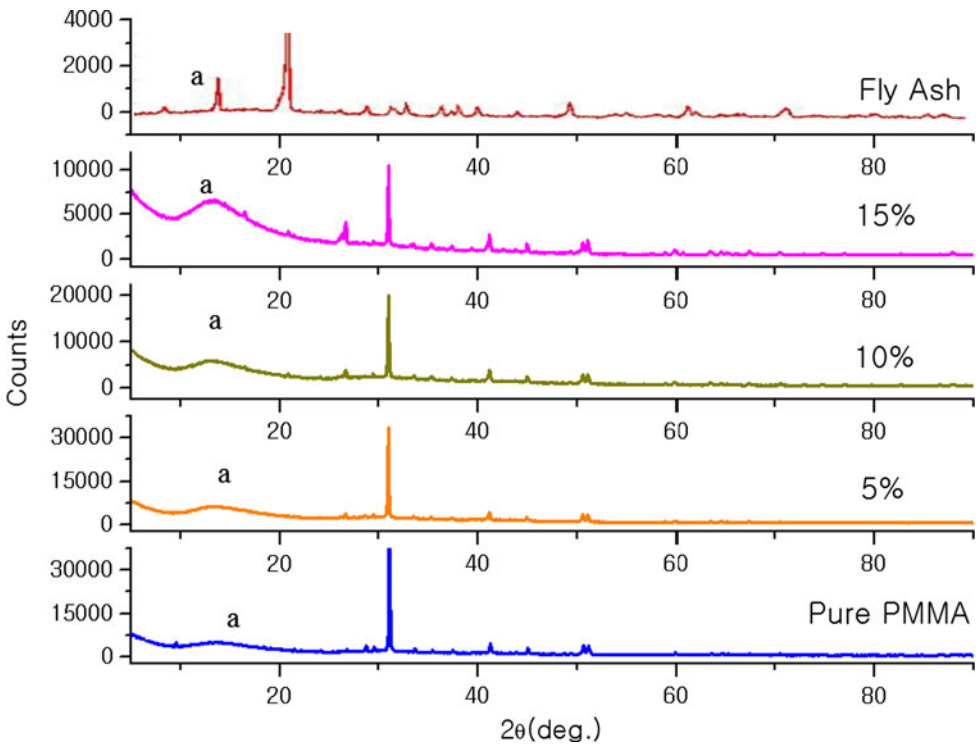

Fig. 4 X-Ray diffraction pattern of pure PMMA, 5% fly ash and PMMA, 10% fly ash and PMMA, 15% fly ash and PMMA

Table 1 Crystallinity, Peaks at 2θ (°), interplaner distance 'd' and crystallite size 'D'(Å) at (1st Peak) point a

S. no	Sample with weight percentage of fly ash (FA)	Crystallinity index or order of crystallinity C_rI (%)	Peaks at 2θ (°)	Interplaner distance 'd' (Å)	Crystallite size 'D' (nm)
1	Pure PMMA	14.00	13.812	6.4152	1.9512
2	5% FA + PMMA	43.04	12.877	6.5508	1.9648
3	10% FA + PMMA	44.57	12.877	6.8749	2.2941
4	15% FA + PMMA	43.72	12.926	6.8489	9.8716

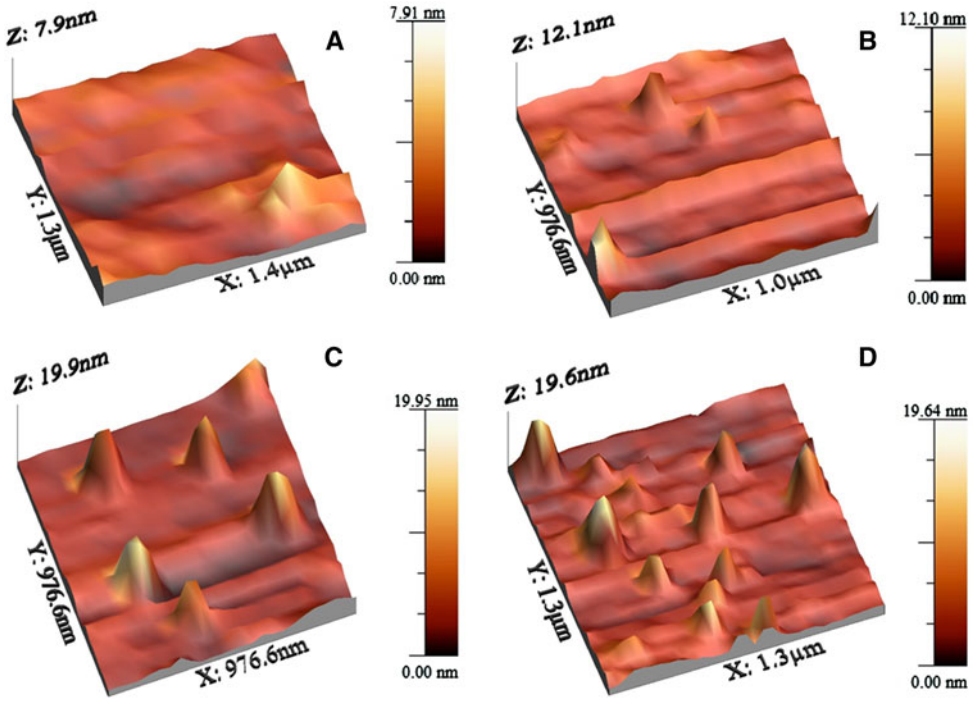

Fig. 5 3D AFM topography of **a** pure PMMA, **b** 5% fly ash and PMMA, **c** 10% fly ash and PMMA, **d** 15% fly ash and PMMA

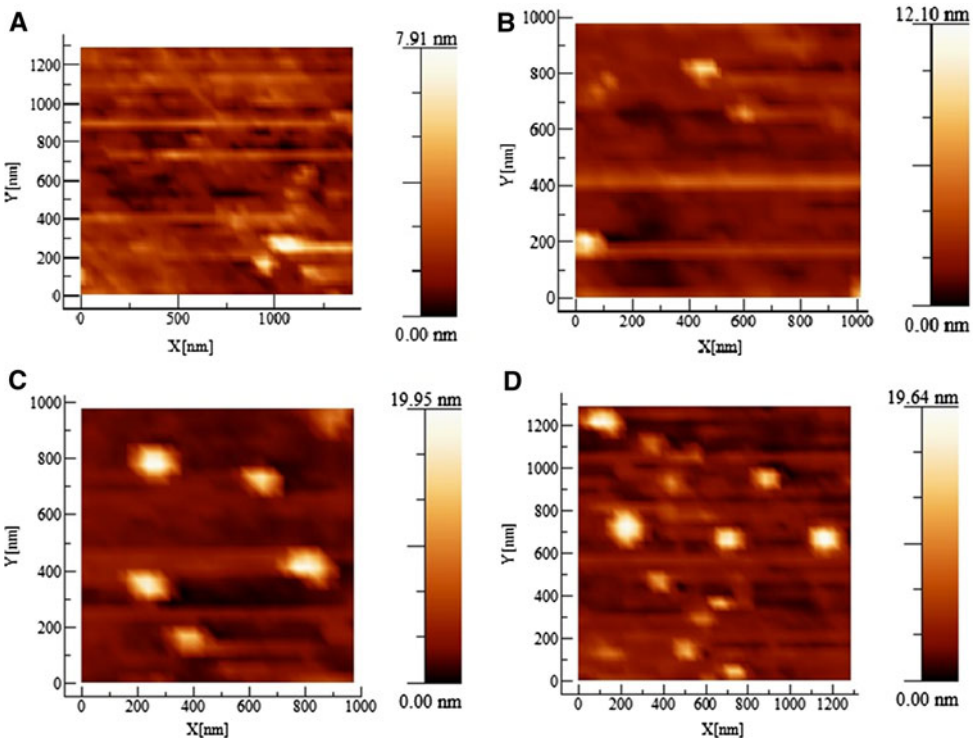

Fig. 6 2D AFM topography of **a** pure PMMA, **b** 5% fly ash and PMMA, **c** 10% fly ash and PMMA, **d** 15% fly ash and PMMA

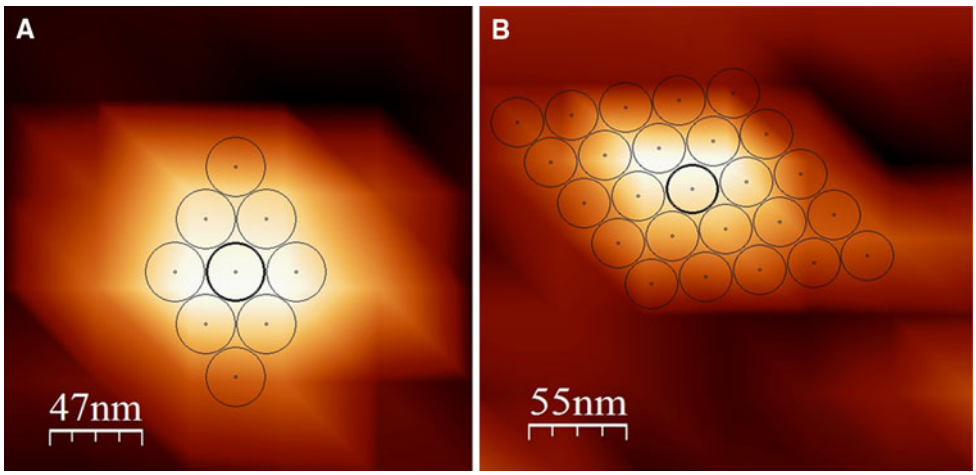

Fig. 7 Bonding of fly ash nanoparticles within the PMMA matrix

As the content of fly ash within the PMMA matrix increases, the number of nano domains is increasing leading to the changes in the properties of PMMA.

4 Conclusion

The outcome of the studies undertaken for the structural, morphological and micromechanical behavior of fly ash reinforced PMMA composite can be formed. The FT-IR studies of pure PMMA and fly ash reinforced PMMA matrix confirms the formation of new peaks and shifting of existing peaks which occurs in the prepared composites thus there is a better linkage of fly ash molecules with PMMA macromolecules, conforming to network structure, confirming the development of stable composites.

The microhardness studies of pure PMMA and prepared composites reveals that the addition of fly ash leads to significant changes in the micro mechanical properties due to modification of structure by interlocking of the chains on the surface and within the fly ash particles. Microhardness increases with increasing concentration of fly ash and size of indent also decreases with increasing fly ash within the PMMA.

The XRD measurement indicates that there is a formation of crystalline region. Crystallinity Index and crystalline size also increases with increasing the concentration of fly ash. The AFM study of pure PMMA and composites confirms the presence of the nanoparticles of fly ash on the surface of the polymer matrix. The qualitative analysis of these images also conform good linkage of these nanoparticles within the PMMA matrix.

All these studies confirms that the addition of fly ash within the PMMA matrix causes the in situ generation of these nanoparticles, which contribute to the enhancement in crystallinity and morphology yielding better micromechanical properties.

Acknowledgments The authors gratefully acknowledge their gratitude to IUC, Indore, India for XRD & AFM analysis and one of the author (A. K. Patel) is thankful to UGC-DAE CSR, Kolkata Centre, India, for financial assistance.

References

Bajpai R, Datt SC (1986) Effect of load on microhardness of polycarbonate. Indian J Pure Appl Phys 24(5):254–255

Bajpai R, Mishra V, Agrawal P, Datt SC (2002) Surface modification on PMMA:PVDF polyblend: hardening under chemical environment. Bull Mater Sci 25(1):21–23

Bajpai R, Dhagat NB, Katare R, Agrawal P, Datt SC (2003a) Development of hardened PVF:PMMA polyblend effect of gamma and electron radiation. Bull Mater Sci 26(4):401–405

Bajpai R, Sharma S, Vastal VK, Chandra BP (2003b) Photoplastic effect in polycarbonate using microhardness measurement. Bull Mater Sci 26(5):537–541

Balamurugan A, Kannan S, Selvaraj V, Rajeswari S (2004) Development and spectral characterization of poly(methyl methacrylate)/hydroxyapatite composite for biomedical applications. Trends Biomater Artif Organs 18(1):41–45

Bartram SF (1967) Hand book of X-ray diffraction, emission, absorption and microscopy. In: Kaelble EF (ed) Chapter-17. McGraw-Hill, New York, pp 17.1–17.12

Celik O, Damci E, Piskin S (2008) Characterization of fly ash and its effects on the compressive strength properties of Portland cement. Indian J Eng Mater Sci 15:433–440

Chand N, Vashishtha SR (2008) Development, structure and strength properties of PP/PMMA/FA blends. Bull Mater Sci 23(2):103–107

Deepa M, Sharma N, Agnihotry SA (2002) FTIR investigations on ion–ion interactions in liquid and gel polymeric electrolytes: LiCF3SO3-PC-PMMA. J Mater Sci 37:1759–1765

Dubey PK, Bajpai R, Keller JM (2008) Structural, morphological and microhardness characterization in polymer complex of laser dye rhodamine (Rh6G) doped polymethyl methacrylate. Microsyst Technol 14:1165–1171

Guo RQ, Rohatgi PK (1998) Chemical reactions between aluminum and fly ash during synthesis and reheating of Al–Fly Ash composite. Metall Mater Trans B V29b:519–525

Gupta AK, Bajpai R, Keller JM (2007) Effect of irradiation on the surface microhardness of pure poly(vinyl fluoride), poly(vinylidene fluoride) and their isomorphic blends. Microsyst Technol 13:589–592

Kalyanasundaram S, Gopalan A, Muniyandi N, Renganathan NG, Saito Y, Kataoka H, Stephan AM, Elizabeth RN (2001) Ionic conductivity, thermal stability and FT-IR studies on plasticized PVC/PMMA blend polymer electrolytes complexed with LiAsF6 and LiPF 6. Ionics 7:44–52

Kumar PRS, Kumaran S, Rao TS, Siivaprasad K (2009) Microstructure and mechanical properties of fly ash particle reinforced AA6061 composites produced by press and extrusion. Trans Indian Inst Metals 62(6):559–566

Ma W, Chen S, Zhang Jn (2009) Crystallization behavior and hydrophilicity of poly(vinylidene fluoride) (PVDF)/poly(methylmethacrylate) (PMMA)/poly(styrene-co-acrylonitrile) (SAN) ternary blends. Colloid Polym Sci 287:147–155

Mas RHMH, Kathiresanb S, Mohanc S (2010) FT-IR and FT-Raman spectra and normal coordinate analysis of poly methyl methacrylate. Der Pharma Chemica 2(4):316–323

Mishra S, Bajpai R, Katare R, Bajpai AK (2007) Radiation induced crosslinking effect on semiinterpenetrating polymer networks of poly(vinyl alcohol). eXPRESS Polym Lett 1(7):407–415

Rabinowetz S, Brown N (1967) Microstrain investigation of polyethylene. J Polym Sci Part A-2: Polym Phys 5(1):143–156

Ramrakhiani M, Parashar P, Datt SC (2005) Study of the degree of crystallinity in eudragit/poly(methyl methacrylate) polyblends by X-ray diffraction. J Appl Polym Sci 96:1835–1838

Rizwan H, Din M (2004) X-ray diffraction study of the changes induced during the thermal digradation of poly (methyl methacrylate) and poly (methacryloyl chloride). Turk J Chem 28:725–729

Ron J (2000) X-ray techniques: overview. In: Mayers RA (ed) Encyclopedia of analytical chemistry. John Wiley and Sons Ltd, Chichester, pp 13269–13288

Statton WO (1967) Hand book of X-ray diffraction, emission, absorption and microscopy. In: Kaelble EF (ed) Chapter-21, McGraw-Hill, New York, pp 21.1–21.19